Demonstration of vortex coronagraph concepts for on-axis telescopes on the Palomar Stellar Double Coronagraph

Dimitri Mawet[a], Chris Shelton[b], James Wallace[b], Michael Bottom[c], Jonas Kuhn[b], Bertrand Mennesson[b], Rick Burruss[b], Randy Bartos[b], Laurent Pueyo[d], Alexis Carlotti[e], and Eugene Serabyn[b]

[a]European Southern Observatory, Alonso de Córdova 3107, Vitacura, Casilla 19001, Chile;
[b]Jet Propulsion Laboratory, California Institute of Technology, Pasadena, CA 91109, USA;
[c]California Institute of Technology, Pasadena, CA 91106, USA;
[d]Space Telescope Science Institute, 3700 San Martin Drive, Baltimore, MD 21218, USA;
[e]Institut de Planétologie et d'Astrophysique de Grenoble (IPAG), University Joseph Fourier, CNRS, BP 53, 38041, Grenoble, France;

ABSTRACT

Here we present preliminary results of the integration of two recently proposed vortex coronagraph (VC) concepts for on-axis telescopes on the Stellar Double Coronagraph (SDC) bench behind PALM-3000, the extreme adaptive optics system of the 200-inch Hale telescope of Palomar observatory. The multi-stage vortex coronagraph (MSVC) uses the ability of the vortex to move light in and out of apertures through multiple VC in series to restore the nominal attenuation capability of the charge 2 vortex regardless of the aperture obscurations. The ring-apodized vortex coronagraph (RAVC) is a one-stage apodizer exploiting the VC Lyot-plane amplitude distribution in order to perfectly null the diffraction from any central obscuration size, and for any vortex topological charge. The RAVC is thus a simple concept that makes the VC immune to diffraction effects of the secondary mirror. It combines a vortex phase mask in the image plane with a single pupil-based amplitude ring apodizer, tailor-made to exploit the unique convolution properties of the VC at the Lyot-stop plane. The prototype apodizer uses the same microdot technology that was used to manufacture the apodized pupil Lyot coronagraph (APLC) equipping SPHERE, GPI and P1640.

Keywords: High contrast imaging, vortex coronagraphy, on-axis telescopes, apodization, Extremely Large Telescopes

1. INTRODUCTION

The vortex coronagraph (VC, see, e.g. Ref. 1) is the most advanced coronagraph currently in operation.[2–4] The VC offers small inner working angle (IWA), down to the diffraction limit ($0.9\lambda/D$), 360° off-axis discovery space, high throughput, achromaticity, operational simplicity, and compatibility with existing classical Lyot coronagraph layouts. It has also recently demonstrated better than 10^{-9} raw contrast levels in the visible on the High Contrast Imaging Testbed (HCIT) at the Jet Propulsion Laboratory.[3,5] The VC has been installed or will be installed in high-contrast imaging instruments of many 5-10 m class telescopes. Since it opens a new parameter space at small separations, it has enabled recent scientific results at Palomar in the H and K bands,[6–9] and at the Very Large Telescope in the L' band.[4,10,11] It is currently being implemented on SCExAO at Subaru (Singh et al. 2014, these proceedings) and on LMIRCAM at the Large Binocular Telescope (Defrère et al. 2014, these proceedings).

As with all other coronagraphs, the VC is sensitive to the aperture geometry, particularly to secondary obscurations.[12,13] This sensitivity stems from the fact that a vortex phase ramp in the focal plane of a telescope always diffracts light to the outer regions of circularly symmetric pupil intensity discontinuities. Thus, as expected, a single vortex will move light outside of the secondary obscuration and support structures, right into

Further author information: send correspondence to dmawet@eso.org

Space Telescopes and Instrumentation 2014: Optical, Infrared, and Millimeter Wave, edited by Jacobus M. Oschmann, Jr., Mark Clampin, Giovanni G. Fazio, Howard A. MacEwen, Proc. of SPIE Vol. 9143, 91432T · © 2014 SPIE
CCC code: 0277-786X/14/$18 · doi: 10.1117/12.2057274

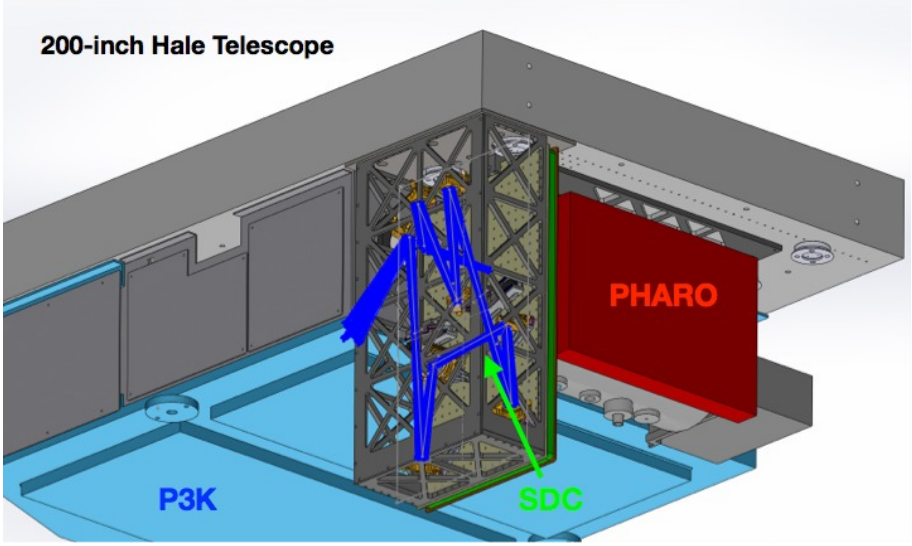

Figure 1. SDC bench CAD drawing, showing its implementation between PALM-3000 and PHARO.

the primary pupil image. The subsequent contrast degradation is proportional to the obscured area $(r_0/R)^2$, with r_0 and R being the radii of the central obscuration and primary mirror, respectively.[12]

In 2011 we proposed a multi-vortex method[13] that reduces this residual light leakage to $(r_0/R)^{2n}$ (n being the number of vortices) without sacrificing throughput. This method enables high contrasts to be reached even with an on-axis telescope, but at the cost of increased optical complexity. More recently, we presented a potentially simpler concept.[14,15] The ring-apodized vortex coronagraph (RAVC) is based on the superposition principle and the vortex properties of moving light in and out of circular apertures. Its principle relies on modulating the entrance pupil with one (or a set of) concentric ring(s) of well chosen size(s) and transmittance(s), in order to yield perfect cancellation of on-axis sources at the Lyot stop level, at the cost of overall throughput (Fogarty et al. 2014, these proceedings, introduced quasi-lossless solutions using remapping techniques). In Ref. 14, we showed that perfect solutions can be found for any topological charge.

2. STELLAR DOUBLE CORONAGRAPH

The Stellar Double Coronagraph (SDC, PI: E. Serabyn) consists of two stages of relay optics between PALM-3000, the Palomar extreme adaptive optics system (R. Dekany et al. 2014, these proceedings) and PHARO, the near-infrared cryogenic imager and spectrograph of the 200-inch Hale telescope. This coronagraph bench features two focal planes and two pupil planes, and can intrinsically accommodate a wide range of coronagraph combinations (vortex, shaped pupil, hybrid Lyot, nextgen apodized Lyot as presented by N'Diaye et al. 2014, these proceedings, etc.) without reconfiguration, and has built-in pupil and image stabilization (image and pupil tracker, and plans for a low-order and high-order wavefront sensor[16]).

The purpose of the SDC is on-sky proof-testing of advanced coronagraphic, wavefront sensing and detector technologies (e.g. MKIDS, see Meeker et al. 2014, these proceedings) in an operational environment (which cannot be simulated). It builds on a bottom-up system-level approach which is critical to future high contrast imaging coronagraphic instruments (for Keck, TMT, and space-based coronagraphs). One crucial feature of the SDC is to enable rich and exciting science while being a fantastic learning experience for the next-generation of coronagraphists.

3. DESIGN, MANUFACTURING, AND VERIFICATION OF THE FIRST RING APODIZER PROTOTYPE

Given the simplicity of the ring apodized masks, and their discrete levels of transmittance, their manufacturing should be straightforward and one can envision using either microdot or optical coating technologies. Here we

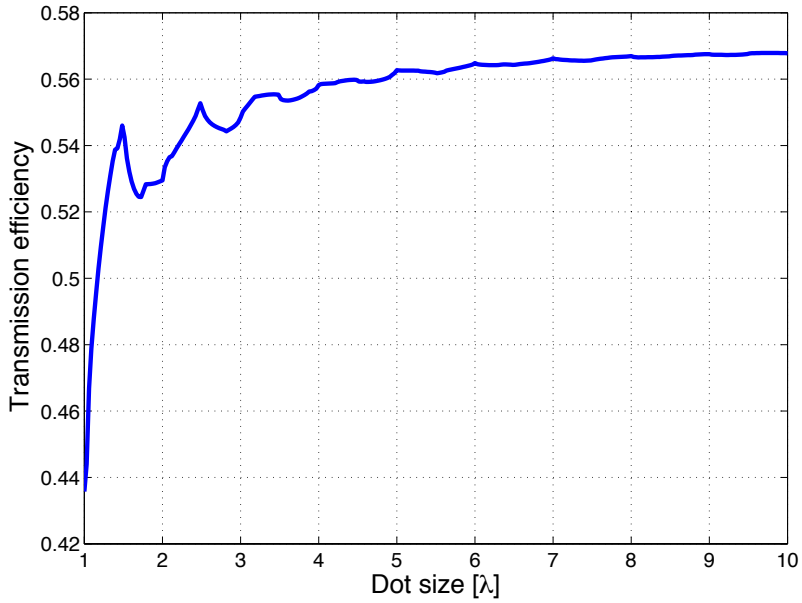

Figure 2. Transmission efficiency as a function of Al dot size (in wavelength units), computed with the RCWA around $\lambda = 1.65$ μm, assuming a $\simeq 45\%$ filled squared grating of Al dots on a CaF_2 substrate.

focus on the well-proven microdot technology, which has been used to fabricate the SPHERE and GPI Apodized Pupil Lyot Coronagraphs.

3.1 Design of the apodizer

The microdot technology, which is well mastered, uses a halftone-dot process, where the relative density of a binary array of pixels (transmission of 0 or 1 at the micron level) is calculated to obtain the required local transmission (here uniform within the rings). The manufacturing of current apodized pupil Lyot coronagraphs[17,18] for SPHERE[19] and GPI[20] uses the microdot technology,[21,22] and the band-limited coronagraphs of NIRCAM soon to fly aboard JWST have also made use of a similar technique.[23] The demonstrated advantages of microdot apodizers are numerous: 1%-level accuracy on the transmission profile, achromatic in phase and amplitude, and compatibility with a wide range of substrate materials and anti-reflective coatings. Spatial phase distortions are in principle absent,[21,22] but careful control will be necessary for the RAVC. Indeed, the perfect superposition of the fields originating from the central obscuration and the ring(s) requires a uniform phase across the apodizer area.

We conducted a trade-off study to determine the optimal dot size for the RAVC apodizer. The dots need to be small enough so as to mitigate diffraction and discretization effects[21,22] but large enough to prevent resonant highly non-linear vectorial diffraction effects. The trade-off therefore boils down to finding the minimum dot size possible before non-scalar diffraction effects kick in. For that, we used the Rigorous Couple Wave Analysis as in Ref. 1, assuming a two-dimensional grating made out of metal (here Al) and air, with a $\simeq 45\%$ filling factor (which corresponds roughly to the design specification of our apodizer). Fig. 2 clearly show that the transmission stabilizes out of resonant effects for dot sizes bigger than $4-5$ the wavelength of impinging light. For this we choose a conservative dot size of 10 μm. Our apodizer is therefore designed for H and K-band use.

We used the error diffusion algorithm for the spatial distribution of the dots. Error diffusion is a well-known half toning technique generating so-called "blue noise" (localized in the frequency space), which follows the following laws:[21,22]

1. Diffraction spots located at $\left(\frac{P}{s}\right)/2 \approx 2100$.

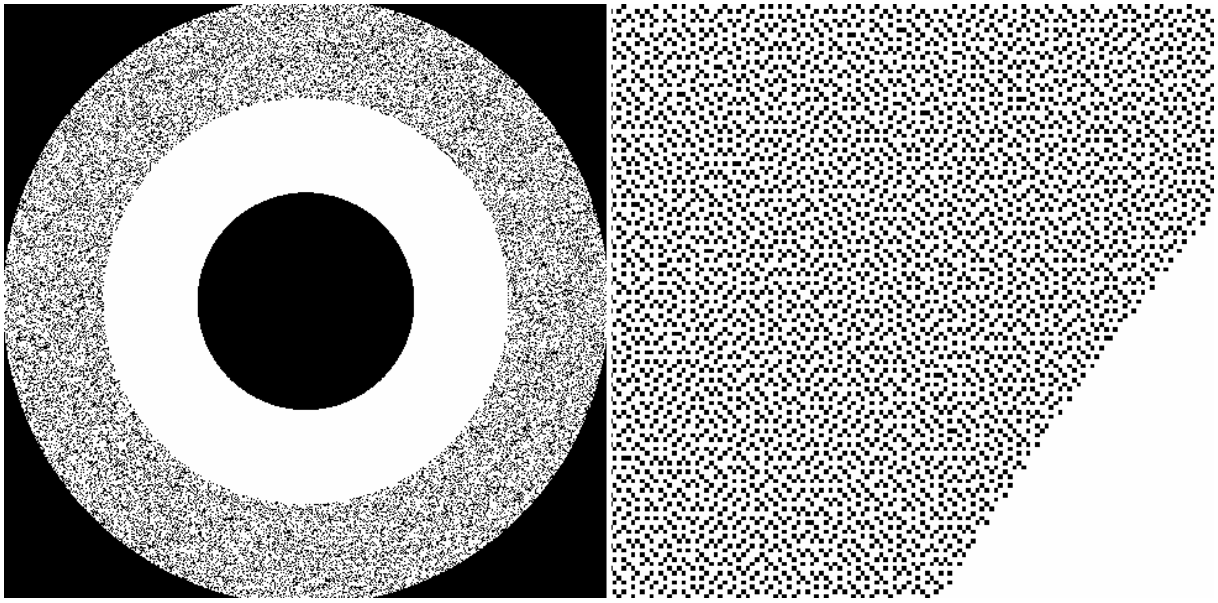

Figure 3. Left: Ring apodizer microdot pattern as specified. The microdots are distributed according to the error diffusion algorithm, creating a well controlled blue noise. Right: Zoom on the microdot pattern showing the result of the error diffusion algorithm.

2. Diffracted intensity equals to $(1-t)\frac{\pi}{4}\left(\frac{s}{P}\right)^2 \approx 8.8 \times 10^{-8}$.

P is the pupil size, and s the dot size. We verified this analytical laws using the Matrix Fourier Transform (MFT), using 8k x 8k entrance pupil array, with 2 pixel per dot, and so a $\frac{P}{s}$ ratio similar to our design choice. We found that the residual contrast level peaks at 1×10^{-8}, which is consistent with the analytical solution.

3.2 Manufacturing of the apodizer prototype

The ring apodizer was manufactured by Photo Sciences, Inc. Its outer diameter is 21.1 mm. The microdot pattern was entirely specified using the error diffusion algorithm (Fig. 3). The microdot are made out of protected Al, deposited on a CaF_2 window, anti-reflective coated with $R < 0.3\%$ from 1.45 μm to 2.45 μm (H and K bands).

3.3 Verification

The ring apodizer was visually inspected for defects, and put under interferometric test (Fig. 4). There is a clear phase step of $\simeq$ 20 nm between the grey and clear rings. We calculated that this phase error is not significant for our infrared application, but would be for future potential use in the visible. This artifact from the microdot technology was not expected and is under investigation.

4. PRELIMINARY RESULTS BEHIND PALM-3000

The SDC has seen its first light on the Hale Telescope in the spring of 2014. The initial observing time was dedicated to fine alignment, optimization of operating modes and early science. Here we only present and discuss preliminary validation tests for the double and ring-apodized vortex coronagraphs. Details of the instrument and first scientific results will be the subjects of forthcoming publications.

4.1 Double vortex preliminary results

Using the white light stimulus of PALM-3000, we took a series of closed loop images in the K band. Fig. 5 (left) shows the images from our series of measurements, off the vortex centers, with the first vortex aligned, and the second one in the beam as well (from left to right). The total starlight suppression we measured within a radius of $4\lambda/D$ (to maximize SNR) is in agreement with theoretical expectations[14] and previous laboratory

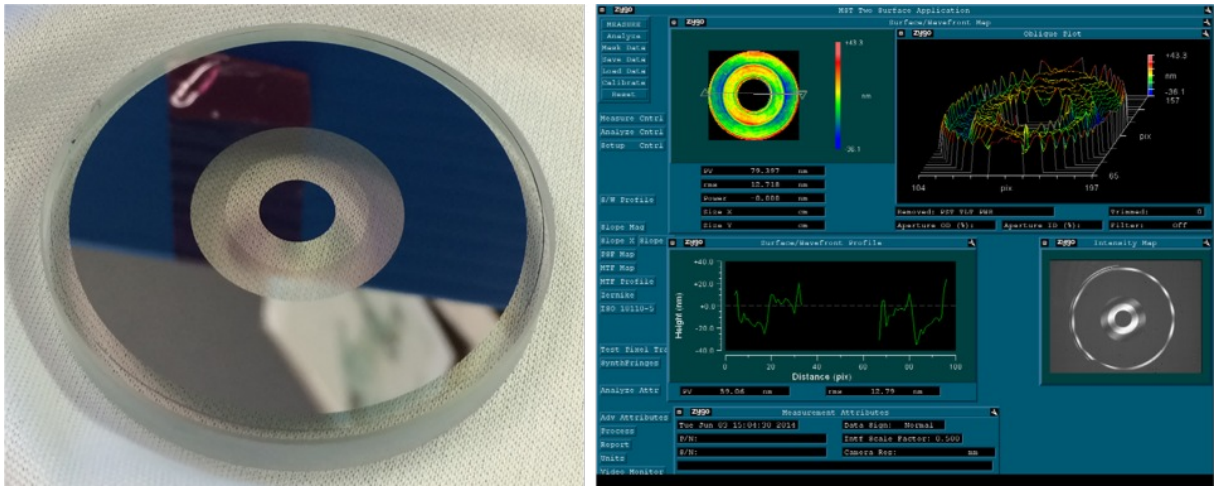

Figure 4. Left: Picture of our ring apodizer prototype, made by Photo Sciences, Inc. out of protected Al microdots on an anti-reflection coated CaF_2 window. Right: IR Zygo interferometric measurement of the ring apodizer, showing the unexpected 20 nm phase step between the gray and clear rings.

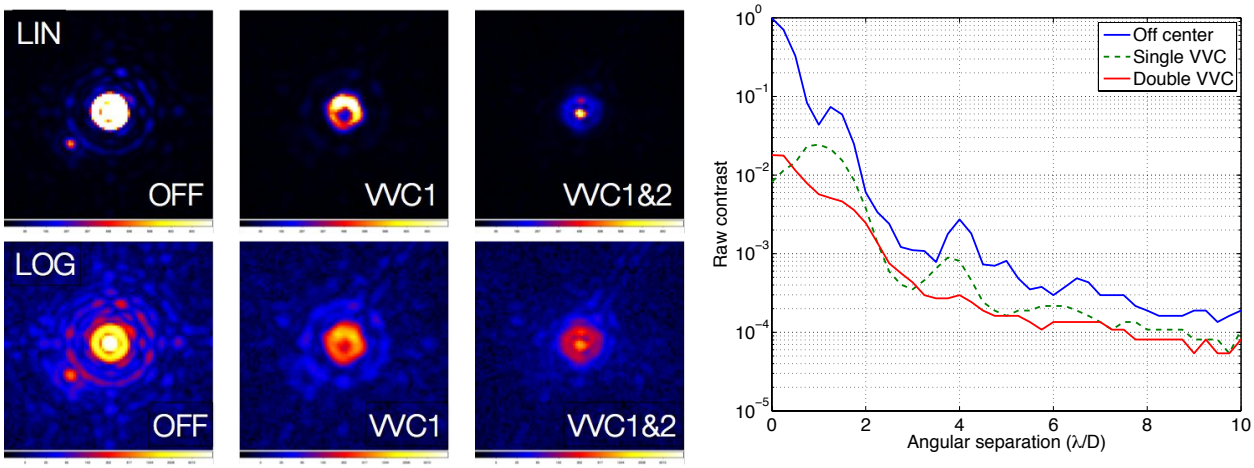

Figure 5. Left: Panel showing the succession of images taken with, from left to right, no vortex, one single vortex, and two vortices in series. The upper panel is in linear scale, showing clearly the peak starlight suppression, and the lower panel is in log scale to show how well the diffraction and pinned speckles are attenuated. Right: Azimuthally averaged intensity profiles of the SDC double vortex coronagraph configuration. Diffraction rings due to the central obscuration are nicely smoothed out in the double VVC (red) curve.

measurements,[24] i.e. $(r_0/R)^2 = 0.36^2 \approx 0.1$ for a single stage, and $(r_0/R)^4 = 0.36^4 \approx 0.02$ for the double stage vortex (Fig. 5, right).

One remarkable feature of the double vortex is the flatness of the residual field at the output pupil of the second vortex, which is a scaled down version of the entrance pupil.[14] This copy of the entrance field should also produce a scaled down version of the entrance PSF, which is what we observe (see Fig. 5, left and right images).

4.2 RAVC proof of concept

We examined the pupil intensity distribution after the SDC charge 2 RAVC, and compared it to our ideal model using a pure vortex. The agreement is qualitatively good, experimentally validating the RAVC concept for the first time (see Fig. 6). Discrepancies can be noted however. We had to remove a αr^2 term first (likely focus), which is not surprising and will be optimized in subsequent tests. Second, there is a drop in expected intensity diffracted outside the pupil (outside of R, so covered by the Lyot stop), which is due to the opaque dot covering the center of our vortex devices.[6,25]

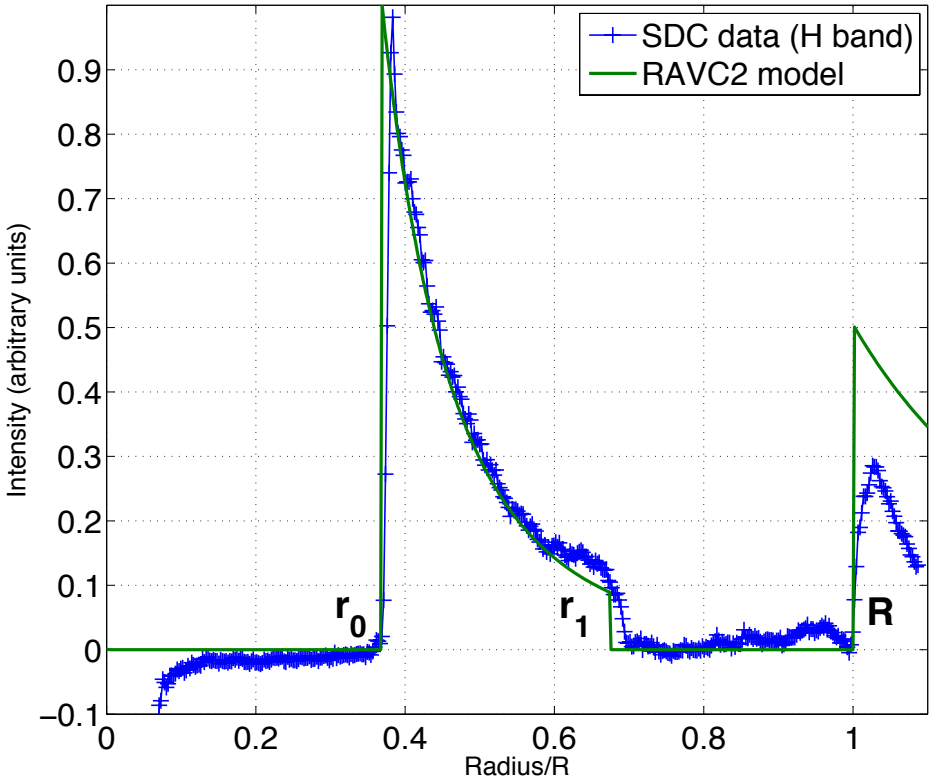

Figure 6. Comparison between the analytical RAVC model for a pure charge 2 vortex and the very first data obtained on the SDC. The match between the model and the data is qualitatively good, even though discrepancies can be noted (see text for details). Following the notation introduced in Ref. 14, we have r_0, the radius of the central obscuration, r_1 the radius of the first apodizer ring, and R the radius of the pupil.

5. CONCLUSIONS AND PERSPECTIVES

We presented preliminary results of the double-stage, and ring-apodized vortex coronagraphs on the Stellar Double Coronagraph of Palomar. Both concepts were originally introduced to solve the sensitivity of the vortex coronagraph to central obscuration, a particularly limiting factor to the use of vortex coronagraph on the 200-inch Hale telescope at Palomar observatory, which has a 36% central obscuration. In this paper, we experimentally demonstrated the validity of both concepts in an operational environment.

The future of the SDC will focus on performance optimization, and the integration of innovative speckle and low-order wavefront sensing techniques,[16] and of course science operations.

ACKNOWLEDGMENTS

This work was carried out at the Jet Propulsion Laboratory, California Institute of Technology, under contract with the National Aeronautics and Space Administration.

REFERENCES

[1] Mawet, D., Riaud, P., Absil, O., and Surdej, J., "Annular Groove Phase Mask Coronagraph," *ApJ* **633**, 1191–1200 (Nov. 2005).

[2] Mawet, D., Murakami, N., Delacroix, C., Serabyn, E., Absil, O., Baba, N., Baudrand, J., Boccaletti, A., Burruss, R., Chipman, R., Forsberg, P., Habraken, S., Hamaguchi, S., Hanot, C., Ise, A., Karlsson, M., Kern, B., Krist, J., Kuhnert, A., Levine, M., Liewer, K., McClain, S., McEldowney, S., Mennesson, B., Moody, D., Murakami, H., Niessner, A., Nishikawa, J., O'Brien, N., Oka, K., Park, P., Piron, P., Pueyo, L., Riaud, P., Sakamoto, M., Tamura, M., Trauger, J., Shemo, D., Surdej, J., Tabirian, N., Traub, W., Wallace, J., and Yokochi, K., "Taking the vector vortex coronagraph to the next level for ground- and space-based exoplanet imaging instruments: review of technology developments in the USA, Japan, and Europe," in [*Society of Photo-Optical Instrumentation Engineers (SPIE) Conference Series*], *Society of Photo-Optical Instrumentation Engineers (SPIE) Conference Series* **8151** (Sept. 2011).

[3] Mawet, D., Pueyo, L., Lawson, P., Mugnier, L., Traub, W., Boccaletti, A., Trauger, J. T., Gladysz, S., Serabyn, E., Milli, J., Belikov, R., Kasper, M., Baudoz, P., Macintosh, B., Marois, C., Oppenheimer, B., Barrett, H., Beuzit, J.-L., Devaney, N., Girard, J., Guyon, O., Krist, J., Mennesson, B., Mouillet, D., Murakami, N., Poyneer, L., Savransky, D., Vérinaud, C., and Wallace, J. K., "Review of small-angle coronagraphic techniques in the wake of ground-based second-generation adaptive optics systems," in [*Proc. SPIE*], **8442** (Sept. 2012).

[4] Mawet, D., Absil, O., Delacroix, C., Girard, J. H., Milli, J., O'Neal, J., Baudoz, P., Boccaletti, A., Bourget, P., Christiaens, V., Forsberg, P., Gonte, F., Habraken, S., Hanot, C., Karlsson, M., Kasper, M., Lizon, J.-L., Muzic, K., Olivier, R., Peña, E., Slusarenko, N., Tacconi-Garman, L. E., and Surdej, J., "L'-band AGPM vector vortex coronagraph's first light on VLT/NACO. Discovery of a late-type companion at two beamwidths from an F0V star," *A&A* **552**, L13 (Apr. 2013).

[5] Serabyn, E., Trauger, J., Moody, D., Mawet, D., Liewer, K., Krist, J., and Kern, B., "High-contrast imaging results with the vortex coronagraph," in [*Society of Photo-Optical Instrumentation Engineers (SPIE) Conference Series*], *Society of Photo-Optical Instrumentation Engineers (SPIE) Conference Series* **8864** (Sept. 2013).

[6] Mawet, D., Serabyn, E., Liewer, K., Burruss, R., Hickey, J., and Shemo, D., "The Vector Vortex Coronagraph: Laboratory Results and First Light at Palomar Observatory," *ApJ* **709**, 53–57 (Jan. 2010).

[7] Mawet, D., Mennesson, B., Serabyn, E., Stapelfeldt, K., and Absil, O., "A Dim Candidate Companion to epsilon Cephei," *ApJl* **738**, L12 (Sept. 2011).

[8] Serabyn, E., Mawet, D., and Burruss, R., "An image of an exoplanet separated by two diffraction beamwidths from a star," *Nature* **464**, 1018–1020 (Apr. 2010).

[9] Wahl, M., Metchev, S. A., Patel, R., Serabyn, G., and PALM-3000 Adaptive Optics Team, "Extreme Contrast Direct Imaging of Planets and Debris disks with the Palomar P3K Adaptive Optics System and the Vector Vortex Coronagraph," in [*American Astronomical Society Meeting Abstracts*], *American Astronomical Society Meeting Abstracts* **221**, 144.22 (Jan. 2013).

[10] Absil, O., Milli, J., Mawet, D., Lagrange, A.-M., Girard, J., Chauvin, G., Boccaletti, A., Delacroix, C., and Surdej, J., "Searching for companions down to 2 AU from β Pictoris using the L'-band AGPM coronagraph on VLT/NACO," *A&A* **559**, L12 (Nov. 2013).

[11] Milli, J., Lagrange, A.-M., Mawet, D., Absil, O., Augereau, J.-C., Mouillet, D., Boccaletti, A., Girard, J. H., and Chauvin, G., "Very deep images of the innermost regions of the beta Pictoris debris disc at Lp," *ArXiv e-prints* (May 2014).

[12] Mawet, D., Pueyo, L., Moody, D., Krist, J., and Serabyn, E., "The Vector Vortex Coronagraph: sensitivity to central obscuration, low-order aberrations, chromaticism, and polarization," in [*Society of Photo-Optical Instrumentation Engineers (SPIE) Conference Series*], *Society of Photo-Optical Instrumentation Engineers (SPIE) Conference Series* **7739** (July 2010).

[13] Mawet, D., Serabyn, E., Wallace, J. K., and Pueyo, L., "Improved high-contrast imaging with on-axis telescopes using a multistage vortex coronagraph," *Optics Letters* **36**, 1506 (Apr. 2011).

[14] Mawet, D., Pueyo, L., Carlotti, A., Mennesson, B., Serabyn, E., and Wallace, J. K., "Ring-apodized Vortex Coronagraphs for Obscured Telescopes. I. Transmissive Ring Apodizers," *ApJSS* **209**, 7 (Nov. 2013).

[15] Mawet, D., Pueyo, L., Carlotti, A., Mennesson, B., Serabyn, E., Wallace, J., and Baudoz, P., "The multistage and ring-apodized vortex coronagraph: two simple, small-angle coronagraphic solutions for heavily obscured apertures," in [*Society of Photo-Optical Instrumentation Engineers (SPIE) Conference Series*], *Society of Photo-Optical Instrumentation Engineers (SPIE) Conference Series* **8864** (Sept. 2013).

[16] Serabyn, E., Wallace, J. K., and Mawet, D., "Speckle-phase measurement in a tandem-vortex coronagraph," *Applied Optics* **50**, 5453 (Oct. 2011).

[17] Soummer, R., "Apodized Pupil Lyot Coronagraphs for Arbitrary Telescope Apertures," *ApJl* **618**, L161–L164 (Jan. 2005).

[18] Soummer, R., Sivaramakrishnan, A., Pueyo, L., Macintosh, B., and Oppenheimer, B. R., "Apodized Pupil Lyot Coronagraphs for Arbitrary Apertures. III. Quasi-achromatic Solutions," *ApJ* **729**, 144 (Mar. 2011).

[19] Kasper, M., Beuzit, J.-L., Feldt, M., Dohlen, K., Mouillet, D., Puget, P., Wildi, F., Abe, L., Baruffolo, A., Baudoz, P., Bazzon, A., Boccaletti, A., Brast, R., Buey, T., Chesneau, O., Claudi, R., Costille, A., Delboulbé, A., Desidera, S., Dominik, C., Dorn, R., Downing, M., Feautrier, P., Fedrigo, E., Fusco, T., Girard, J., Giro, E., Gluck, L., Gonte, F., Gojak, D., Gratton, R., Henning, T., Hubin, N., Lagrange, A.-M., Langlois, M., Mignant, D. L., Lizon, J.-L., Lilley, P., Madec, F., Magnard, Y., Martinez, P., Mawet, D., Mesa, D., Müller-Nilsson, O., Moulin, T., Moutou, C., O'Neal, J., Pavlov, A., Perret, D., Petit, C., Popovic, D., Pragt, J., Rabou, P., Rochat, S., Roelfsema, R., Salasnich, B., Sauvage, J.-F., Schmid, H. M., Schuhler, N., Sevin, A., Siebenmorgen, R., Soenke, C., Stadler, E., Suarez, M., Turatto, M., Udry, S., Vigan, A., and Zins, G., "Gearing up the SPHERE," *The Messenger* **149**, 17–21 (Sept. 2012).

[20] Macintosh, B. A., Graham, J. R., Palmer, D. W., Doyon, R., Dunn, J., Gavel, D. T., Larkin, J., Oppenheimer, B., Saddlemyer, L., Sivaramakrishnan, A., Wallace, J. K., Bauman, B., Erickson, D. A., Marois, C., Poyneer, L. A., and Soummer, R., "The Gemini Planet Imager: from science to design to construction," *Adaptive Optics Systems. Edited by Hubin* **7015**, 31 (July 2008).

[21] Martinez, P., Dorrer, C., Aller Carpentier, E., Kasper, M., Boccaletti, A., Dohlen, K., and Yaitskova, N., "Design, analysis, and testing of a microdot apodizer for the Apodized Pupil Lyot Coronagraph," *A&A* **495**, 363–370 (Feb. 2009).

[22] Martinez, P., Dorrer, C., Kasper, M., Boccaletti, A., and Dohlen, K., "Design, analysis, and testing of a microdot apodizer for the apodized pupil Lyot coronagraph. II. Impact of the dot size," *A&A* **500**, 1281–1285 (June 2009).

[23] Krist, J. E., Balasubramanian, K., Beichman, C. A., Echternach, P. M., Green, J. J., Liewer, K. M., Muller, R. E., Serabyn, E., Shaklan, S. B., Trauger, J. T., Wilson, D. W., Horner, S. D., Mao, Y., Somerstein, S. F., Vasudevan, G., Kelly, D. M., and Rieke, M. J., "The JWST/NIRCam coronagraph: mask design and fabrication," in [*Society of Photo-Optical Instrumentation Engineers (SPIE) Conference Series*], *Society of Photo-Optical Instrumentation Engineers (SPIE) Conference Series* **7440** (Aug. 2009).

[24] Serabyn, E., Mawet, D., Wallace, J. K., Liewer, K., Trauger, J., Moody, D., and Kern, B., "Recent progress in vector vortex coronagraphy," in [*Society of Photo-Optical Instrumentation Engineers (SPIE) Conference Series*], *Society of Photo-Optical Instrumentation Engineers (SPIE) Conference Series* **8146** (Sept. 2011).

[25] Mawet, D., Serabyn, E., Liewer, K., Hanot, C., McEldowney, S., Shemo, D., and O'Brien, N., "Optical Vectorial Vortex Coronagraphs using Liquid Crystal Polymers: theory, manufacturing and laboratory demonstration," *Optics Express* **17**, 1902–1918 (Feb. 2009).